

DYNAMICAL ELECTROWEAK SYMMETRY BREAKING: IMPLICATIONS OF THE H^0

Updated October 2015 by R.S. Chivukula (Michigan State University), M. Narain (Brown University), and J. Womersley (STFC, Rutherford Appleton Laboratory).

1. Introduction and Phenomenology

In theories of dynamical electroweak symmetry breaking, the electroweak interactions are broken to electromagnetism by the vacuum expectation value of a composite operator, typically a fermion bilinear. In these theories, the longitudinal components of the massive weak bosons are identified with composite Nambu-Goldstone bosons arising from dynamical symmetry breaking in a strongly-coupled extension of the standard model. Viable theories of dynamical electroweak symmetry breaking must also explain (or at least accommodate) the presence of an additional composite scalar state to be identified with the H^0 scalar boson [1,2] – a state unlike any other observed to date.

Theories of dynamical electroweak symmetry breaking can be classified by the nature of the composite singlet state to be associated with the H^0 , and the corresponding dimensional scales f , the analog of the pion decay-constant in QCD, and Λ , the scale of the underlying strong dynamics.¹ Of particular importance is the ratio v/f , where $v^2 = 1/(\sqrt{2}G_F) \approx (246 \text{ GeV})^2$, since this ratio measures the expected size of the deviations of the couplings of a composite Higgs boson from those expected in the standard model. The basic possibilities, and the additional states that they predict, are described below.

1.1 Technicolor, $v/f \simeq 1$, $\Lambda \simeq 1 \text{ TeV}$:

Technicolor models [8–10] incorporate a new asymptotically free gauge theory (“technicolor”) and additional massless fermions (“technifermions” transforming under a vectorial representation of the gauge group). The global chiral symmetry of the fermions is spontaneously broken by the formation of a

¹ In a strongly interacting theory “Naive Dimensional Analysis” [3,4] implies that, in the absence of fine-tuning, $\Lambda \simeq g^* f$ where $g^* \simeq 4\pi$ is the typical size of a strong coupling in the low-energy theory [5,6]. This estimate is modified in the presence of multiple flavors or colors [7].

technifermion condensate, just as the approximate chiral symmetry in QCD is broken down to isospin by the formation of a quark condensate. The $SU(2)_W \times U(1)_Y$ interactions are embedded in the global technifermion chiral symmetries in such a way that the only unbroken gauge symmetry after chiral symmetry breaking is $U(1)_{em}$.² These theories naturally provide the Nambu-Goldstone bosons “eaten” by the W and Z boson. There would also typically be additional heavy states (e.g. vector mesons, analogous to the ρ and ω mesons in QCD) with TeV masses [14,15], and the WW and ZZ scattering amplitudes would be expected to be strong at energies of order 1 TeV.

There are various possibilities for the scalar H^0 in technicolor models, as described below.³ In all of these cases, however, to the extent that the H^0 has couplings consistent with those of the standard model, these theories are very highly constrained.

a) **H^0 as a singlet scalar resonance:** The strongly-interacting fermions which make up the Nambu-Goldstone bosons eaten by the weak bosons would naturally be expected to also form an isoscalar neutral bound state, analogous to the σ particle expected in pion-scattering in QCD [16]. However, in this case, there is no symmetry protecting the mass of such a particle – which would therefore generically be of order the energy scale of the underlying strong dynamics Λ . In the simplest theories of this kind – those with a global $SU(2)_L \times SU(2)_R$ chiral symmetry which is spontaneously broken to $SU(2)_V$ – the natural dynamical scale Λ would be of order a TeV, resulting in a particle too heavy and broad to be identified with the H^0 . The scale of the underlying interactions could naturally be smaller than 1 TeV if the global symmetries of the theory are larger than $SU(2)_L \times SU(2)_R$, but in this case there would be additional (pseudo-)Nambu-Goldstone bosons (more on this below). A theory of this kind would only be viable, therefore, if some choice of the parameters of the high energy theory could

² For a review of technicolor models, see [11–13].

³ In these models, the self-coupling of the H^0 scalar is not related to its mass, as it is in the SM – though there are currently no experimental constraints on this coupling.

give rise to sufficiently light state without the appearance of additional particles that should have already been observed. Furthermore, while a particle with these quantum numbers could have Higgs-like couplings to any electrically neutral spin-zero state made of quarks, leptons, or gauge-bosons, there is no symmetry insuring that the coupling strengths of such a composite singlet scalar state would be precisely the same as those of the standard model Higgs [17].

b) **H⁰ as a dilaton:** It is possible that the underlying strong dynamics is approximately scale-invariant, as inspired by theories of “walking technicolor” [18–22], and that both the scale and electroweak symmetries are spontaneously broken at the TeV energy scale [23]. In this case, due to the spontaneous breaking of approximate scale invariance, one might expect a corresponding (pseudo-) Nambu-Goldstone boson [19] with a mass less than a TeV, the dilaton.⁴ A dilaton couples to the trace of the energy momentum tensor, which leads to a similar pattern of two-body couplings as the couplings of the standard model Higgs boson [28–30]. Scale-invariance is a space-time symmetry, however, and is unrelated to the global symmetries that we can identify with the electroweak group. Therefore the decay-constants associated with the breaking of the scale and electroweak symmetries will not, in general, be the same.⁵ In other words, if there are no large anomalous dimensions associated with the W - and Z -bosons or the top- or bottom-quarks, the ratios of the couplings of the dilaton to these particles would be the same as the ratios of the same couplings for the standard model Higgs boson, but the overall strength of the dilaton couplings would be expected to be different [31,32]. Furthermore, the couplings of the dilaton to gluon- and photon-pairs can be related to the

⁴ Even in this case, however, a dilaton associated with electroweak symmetry breaking will likely not *generically* be as light as the H⁰ [24–27].

⁵ If both the electroweak symmetry and the approximate scale symmetry are broken only by electroweak doublet condensate(s), then the decay-constants for scale and electroweak symmetry breaking may be approximately equal – differing only by terms formally proportional to the amount of explicit scale-symmetry breaking.

beta functions of the corresponding gauge interactions in the underlying high-energy theory, and will not in general yield couplings with the exactly the same strengths as the standard model [33,34].

- c) **H⁰ as a singlet Pseudo-Nambu-Goldstone Boson:** If the global symmetries of the technicolor theory are larger than $SU(2)_L \times SU(2)_R$, there can be extra singlet (pseudo-) Nambu-Goldstone bosons which could be identified with the H⁰. In this case, however, the coupling strength of the singlet state to WW and ZZ pairs would be comparable to the couplings to gluon and photon pairs, and these would all arise from loop-level couplings in the underlying technicolor theory [35]. This pattern of couplings is not supported by the data.

1.2 The Higgs doublet as a pseudo-Nambu-Goldstone Boson, $v/f < 1$, $\Lambda > 1$ TeV:

In technicolor models, the symmetry-breaking properties of the underlying strong dynamics necessarily breaks the electroweak gauge symmetries. An alternative possibility is that the underlying strong dynamics itself does not break the electroweak interactions, and that the entire quartet of bosons in the Higgs doublet (including the state associated with the H⁰) are composite (pseudo-) Nambu-Goldstone particles [36,37]. In this case, the underlying dynamics can occur at energies larger than 1 TeV and additional interactions with the top-quark mass generating sector (and possibly with additional weakly-coupled gauge bosons) cause the vacuum energy to be minimized when the composite Higgs doublet gains a vacuum expectation value [38,39]. In these theories, the couplings of the remaining singlet scalar state would naturally be equal to that of the standard model Higgs boson up to corrections of order $(v/f)^2$ and, therefore, constraints on the size of deviations of the H⁰ couplings from that of the standard model Higgs give rise to lower bounds on the scales f and Λ .⁶

⁶ In these models v/f is an adjustable parameter, and in the limit $v/f \rightarrow 1$ they reduce, essentially, to the technicolor models discussed in the previous subsection. Our discussion here is consistent with that given there, since we expect corrections to the SM Higgs couplings to be large for $v/f \simeq 1$.

The electroweak gauge interactions, as well as the interactions responsible for the top-quark mass, explicitly break the chiral symmetries of the composite Higgs model, and lead generically to sizable corrections to the mass-squared of the Higgs-doublet – the so-called “Little Hierarchy Problem” [40]. “Little Higgs” theories [41–44] are examples of composite Higgs models in which the (collective) symmetry-breaking structure is selected so as to suppress these contributions to the Higgs mass-squared.

Composite Higgs models typically require a larger global symmetry of the underlying theory, and hence additional relatively light (compared to Λ) scalar particles, extra electroweak vector bosons (e.g. an additional $SU(2) \times U(1)$ gauge group), and vector-like partners of the top-quark of charge $+2/3$ and possibly also $+5/3$ [45]. Finally, in addition to these states, one would expect the underlying dynamics to yield additional scalar and vector resonances with masses of order Λ . If the theory respects a custodial symmetry [46], the couplings of these additional states to the electroweak and Higgs boson will be related – and, for example, one might expect a charged vector resonance to have similar branching ratios to WZ and WH . Different composite Higgs models utilize different mechanisms for arranging for the hierarchy of scales $v < f$ and arranging for a scalar Higgs self-coupling small enough to produce an H^0 of mass of order 125 GeV, for a review see [48].

1.3 Top-Condensate, Top-Color, Top-Seesaw and related theories, $v/f < 1$, $\Lambda > 1$ TeV:

A final alternative is to consider a strongly interacting theory with a high (compared to a TeV) underlying dynamical scale that *would* naturally break the electroweak interactions, but whose strength is adjusted (“fine-tuned”) to produce electroweak symmetry breaking at 1 TeV. This alternative is possible if the electroweak (quantum) phase transition is continuous (second order) in the strength of the strong dynamics [47]. If the fine tuning can be achieved, the underlying strong interactions will produce a light composite Higgs bound state with couplings equal to that of the standard model Higgs boson up to corrections of order $(1 \text{ TeV}/\Lambda)^2$. As in theories in which

electroweak symmetry breaking occurs through vacuum alignment, therefore, constraints on the size of deviations of the H^0 couplings from that of the standard model Higgs give rise to lower bounds on the scale Λ . Formally, in the limit $\Lambda \rightarrow \infty$ (a limit which requires arbitrarily fine adjustment of the strength of the high-energy interactions), these theories are equivalent to a theory with a fundamental Higgs boson – and the fine adjustment of the coupling strength is a manifestation of the hierarchy problem of theories with a fundamental scalar particle.

In many of these theories the top-quark itself interacts strongly (at high energies), potentially through an extended color gauge sector [49–53]. In these theories, top-quark condensation (or the condensation of an admixture of the top with additional vector-like quarks) is responsible for electroweak symmetry breaking, and the H^0 is identified with a bound state involving the third generation of quarks. These theories typically include an extra set of massive color-octet vector bosons (top-gluons), and an extra $U(1)$ interaction (giving rise to a top-color Z') which couple preferentially to the third generation and whose masses define the scale Λ of the underlying physics.

1.4 Flavor

In addition to the electroweak symmetry breaking dynamics described above, which gives rise to the masses of the W and Z particles, additional interactions must be introduced to produce the masses of the standard model fermions. Two general avenues have been suggested for these new interactions. In one case, e.g. “extended technicolor” (ETC) theories [54,55], the gauge interactions in the underlying strongly interacting theory are extended to incorporate flavor. This extended gauge symmetry is broken down (possibly sequentially, at several different mass scales) to the residual strongly-interacting interaction responsible for electroweak symmetry breaking. The massive gauge-bosons corresponding to the broken symmetries then mediate interactions between mass operators for the quarks/leptons and the corresponding bilinears of the strongly-interacting fermions, giving rise to the masses of the ordinary fermions after electroweak symmetry breaking. An alternative proposal, “partial compositeness” [56], the additional

interactions giving rise to mixing between the ordinary quarks and leptons and massive composite fermions in the strongly-interacting underlying theory. Theories incorporating partial compositeness include additional vector-like partners of the ordinary quarks and leptons, typically with masses of order a TeV or less.

In both cases, the effects of these flavor interactions on the electroweak properties of the ordinary quarks and leptons are likely to be most pronounced in the third generation of fermions.⁷ The additional particles present, especially the additional scalars, often couple more strongly to heavier fermions.

Moreover, since the flavor interactions must give rise to quark mixing, we expect that a generic theory of this kind could give rise to large flavor-changing neutral-currents [55]. In ETC theories, these constraints are typically somewhat relaxed if the theory incorporates approximate generational flavor symmetries [57], the theory “walks” [18–22], or if $\Lambda > 1$ TeV [58]. In theories of partial compositeness, the masses of the ordinary fermions depend on the scaling-dimension of the operators corresponding to the composite fermions with which they mix. This leads to a new mechanism for generating the mass-hierarchy of the observed quarks and leptons that, potentially, ameliorates flavor-changing neutral current problems and can provide new contributions to the composite Higgs potential which allows for $v/f < 1$ [59–63].

Alternatively, one can assume that the underlying flavor dynamics respects flavor symmetries (“minimal” [64,65] or “next-to-minimal” [66] flavor violation) which suppress flavor-changing neutral currents in the two light generations. Additional considerations apply when extending these considerations to potential explanation of neutrino masses (see, for example, [67,68]) .

Since the underlying high-energy dynamics in these theories are strongly coupled, there are no reliable calculation techniques that can be applied to analyze their properties. Instead, most

⁷ Indeed, from this point of view, the vector-like partners of the top-quark in top-seesaw and little Higgs models can be viewed as incorporating partial compositeness to explain the origin of the top quark’s large mass.

phenomenological studies depend on the construction of a “low-energy” effective theory describing additional scalar, fermion, or vector boson degrees of freedom, which incorporates the relevant symmetries and, when available, dynamical principles. In some cases, motivated by the AdS/CFT correspondence [69], the strongly-interacting theories described above have been investigated by analyzing a dual compactified five-dimensional gauge theory. In these cases, the AdS/CFT “dictionary” is used to map the features of the underlying strongly coupled high-energy dynamics onto the low-energy weakly coupled dual theory [70].

More recently, progress has been made in investigating strongly-coupled models using lattice gauge theory [71–73]. These calculations offer the prospect of establishing which strongly coupled theories of electroweak symmetry breaking have a particle with properties consistent with those observed for the H^0 – and for establishing concrete predictions for these theories at the LHC [74].

2. Experimental Searches

As discussed above, the extent to which the couplings of the H^0 conform to the expectations for a standard model Higgs boson constrains the viability of each of these models. Measurements of the H^0 couplings, and their interpretation in terms of effective field theory, are summarized in the H^0 review in this volume. In what follows, we will focus on searches for the additional particles that might be expected to accompany the singlet scalar: extra scalars, fermions, and vector bosons. In some cases, detailed model-specific searches have been made for the particles described above (though generally not yet taking account of the demonstrated existence of the H^0 boson).

In most cases, however, generic searches (e.g. for extra W' or Z' particles, extra scalars in the context of multi-Higgs models, or for fourth-generation quarks) are quoted that can be used – when appropriately translated – to derive bounds on a specific model of interest.

The mass scale of the new particles implied by the interpretations of the low mass of H^0 discussed above, and existing studies from the Tevatron and lower-energy colliders, suggests

that only the Large Hadron Collider has any real sensitivity. A number of analyses already carried out by ATLAS and CMS use relevant final states and might have been expected to observe a deviation from standard model expectations – in no case so far has any such deviation been reported. The detailed implications of these searches in various model frameworks are described below.

Except where otherwise noted, all limits in this section are quoted at a confidence level of 95%. The ATLAS searches have analyzed 20.3 fb^{-1} of data recorded at the LHC with $\sqrt{s}=8 \text{ TeV}$, and the CMS analyses are based on the data collected at $\sqrt{s} = 8 \text{ TeV}$ in 2012 with an integrated luminosity of 19.7 fb^{-1} .

2.1 Searches for Z' or W' Bosons

Massive vector bosons or particles with similar decay channels would be expected to arise in Little Higgs theories, in theories of Technicolor, or models involving a dilaton, adjusted to produce a light Higgs boson, consistent with the observed H^0 . These particles would be expected to decay to pairs of vector bosons, to third generation quarks, or to leptons. The generic searches for W' and Z' vector bosons listed below can, therefore, be used to constrain models incorporating a composite Higgs-like boson.

$Z' \rightarrow \ell\ell$:

ATLAS [76] and CMS [77] have both searched for Z' production with $Z' \rightarrow ee$ or $\mu\mu$. The main backgrounds to these analyses arise from Drell-Yan, $t\bar{t}$, and diboson production and are estimated using Monte Carlo simulation, with the cross sections scaled by next-to-next-to-leading-order k -factors. Instrumental backgrounds from QCD multijet and W +jet events are estimated using control data samples. No deviation from the standard model prediction is seen in the dielectron and dimuon invariant mass spectra, by either the ATLAS or the CMS analysis, and lower limits on possible Z' boson masses are set. The dielectron channel has higher sensitivity due to the superior mass resolution compared to the dimuon channel. A Z'_{SSM} with couplings equal to the standard model Z (a “sequential standard model” Z') and a mass below 2.79 TeV

is excluded by ATLAS, while CMS sets a lower mass limit of 2.90 TeV. The ATLAS analysis rules out various $E6$ -motivated bosons (Z'_ψ, Z'_χ) and Z^* with masses lower than 2.51, 2.62 and 2.85 TeV, while a Z'_ψ with a mass below 2.57 TeV is excluded by CMS. The experiments also place limits on the parameters of extra dimension models and in the case of ATLAS on the parameters of a minimal walking technicolor model [18–22], consistent with a 125 GeV Higgs boson.

In addition, both experiments have also searched for Z' decaying to a ditau final state [78,79]. While less sensitive than dielectron or dimuon final states, an excess in $\tau^+\tau^-$ could have interesting implications for models in which lepton universality is not a necessary requirement and enhanced couplings to the third generation are allowed. This analysis leads to lower limits on the mass of a Z'_{SSM} of 2.0 and 1.3 TeV from ATLAS and CMS respectively.

$Z' \rightarrow q\bar{q}$:

The ability to relatively cleanly select $t\bar{t}$ pairs at the LHC together with the existence of enhanced couplings to the third generation in many models makes it worthwhile to search for new particles decaying in this channel. Both ATLAS [80] and CMS [81] have carried out searches for new particles decaying into $t\bar{t}$. ATLAS focuses on the lepton plus jets final state, where the top quark pair decays as $t\bar{t} \rightarrow WbWb$ with one W boson decaying leptonically and the other hadronically; CMS uses final states where both, one or neither W decays leptonically and then combines the results. The $t\bar{t}$ invariant mass spectrum is analyzed for any excess, and no evidence for any resonance is seen. ATLAS excludes a narrow ($\Gamma/m = 1.2\%$) leptophobic top-color Z' boson with a mass below 1.8 TeV; upper limits are set on the cross section times branching ratio for a broad color octet resonance with $\Gamma/m = 15\%$ decaying to $t\bar{t}$ which range from 4.8 pb for $m = 0.4$ TeV to 0.09 pb for $m = 3.0$ TeV. CMS sets limits on a narrow ($\Gamma/m = 1.2\%$) Z' boson decaying to $t\bar{t}$ of 2.4 TeV and on a wide resonance (10% width) of 2.8 TeV. In the Randall-Sundrum model, KK gravitons (g_{KK}) with masses below 2.2 TeV are excluded by ATLAS and (for a different set of model parameters) below 2.7 TeV by CMS.

Both ATLAS [82] and CMS [83] have also searched for resonances decaying into $q\bar{q}$, qg or gg using the dijet invariant mass spectrum. Model-independent upper limits on cross sections are set; ATLAS excludes color-octet scalars below 2.72 TeV, W' bosons below 2.45 TeV and chiral W^* bosons below 1.75 TeV. CMS is able to exclude W' bosons below 1.9 TeV or between 2.0 and 2.2 TeV; Z' bosons below 1.7 TeV; and g_{KK} gravitons below 1.6 TeV. Searches are also carried out for wide resonances, assuming Γ/m up to 30%, and exclude axigluons and colorons with mass below 3.6 TeV, and color-octet scalars with mass below 2.5 TeV.

$W' \rightarrow \ell\nu$:

Both LHC experiments have also searched for massive charged vector bosons. ATLAS [85] searched for a heavy W' decaying to $e\nu$ or $\mu\nu$ and find no excess over the standard model expectation. A sequential standard model W' (assuming zero branching ratio to WZ) with mass less than 3.24 TeV is excluded, and excited chiral bosons W^* excluded up to 3.21 TeV.

CMS [86] has carried out a complementary search in the $\tau\nu$ final state. As noted above, such searches place interesting limits on models with enhanced couplings to the third generation. No excess is observed and limits between 2.0 and 2.7 TeV are set on the mass of a W' decaying preferentially to the third generation; a W' with universal fermion couplings is also excluded for masses less than 2.7 TeV.

$W' \rightarrow t\bar{b}$:

Heavy new gauge bosons can couple to left-handed fermions like the W boson or to right-handed fermions. W' bosons that couple only to right-handed fermions may not have leptonic decay modes, depending on the mass of the right-handed neutrino. For these W' bosons, the $t\bar{b}$ decay mode is especially important because it is the hadronic decay mode with the best signal-to-background.

ATLAS has searched for W' bosons in the $t\bar{b}$ final state both for leptonic [87] and hadronic [88] decays of the top. No significant deviations from the standard model are seen in either analysis and limits are set on the $W' \rightarrow t\bar{b}$ cross section times

branching ratio and on the W' effective couplings. W' bosons with purely left-handed (right-handed) couplings to fermions are excluded for masses below 1.70 (1.92) TeV.

2.2 Searches for Resonances decaying to Vector Bosons and/or Higgs Bosons

$X \rightarrow WW, WZ, ZZ$:

Both experiments have used the data collected at $\sqrt{s} = 8$ TeV to search for resonances decaying to pairs of bosons.

ATLAS [89] and CMS [90] have both looked for a resonant state (such as a W') decaying to WZ in the fully-leptonic channel, $\ell\nu\ell'\ell'$ (where $\ell, \ell' = e, \mu$). The WZ invariant mass distribution reconstructed from the observed lepton momenta missing transverse energy. The backgrounds arise mainly from standard model WZ , ZZ and $t\bar{t} + W/Z$ production. No significant deviation from the standard model prediction is observed by either experiment. A W' with mass less than 1.55 (1.52) TeV is excluded by CMS (ATLAS); ATLAS also sets limits on the production cross section for heavy vector triplet particles, and CMS sets limits on the production of low-scale technimesons ρ_{TC} from the reconstructed WZ mass spectrum and cross section.

ATLAS [91,92] and CMS [93] have also searched for narrow resonances decaying to WW , WZ or ZZ in $\ell\nu jj$ and $\ell\ell jj$ final states (where one boson decays leptonically and the other to jets). No deviation from the standard model is seen by either experiment; resonance masses below 1.59 TeV for an extended gauge model W' are excluded by ATLAS. CMS interprets their results in terms of Randall-Sundrum g_{KK} production but also presents model-independent cross section limits that can be used to constrain other models.

Searches have also been conducted in fully hadronic final states. ATLAS [94] and CMS [95] have searched for massive resonance in dijet systems with one or both jets identified as a W or a Z boson using jet-substructure techniques. ATLAS observes a small excess (less than three standard deviations) around 2 TeV in the WZ channel but otherwise no deviations from the standard model are seen. Limits are set by both experiments on the production cross section times branching

ratio for new heavy W' decaying to WZ and for g_{KK} gravitons decaying to WW or ZZ . CMS also sets limits on the production of particles decaying to qW and qZ .

$X \rightarrow W/Z + H^0$ and $X \rightarrow H^0 H^0$:

With the existence and decay properties of the Higgs boson established, and the significant datasets now available, it is possible to use searches for anomalous production of the Higgs as a potential signature for new physics. ATLAS [96] and CMS [97,98] have both searched in the data collected at $\sqrt{s} = 8$ TeV for new particles decaying to a vector boson plus a Higgs boson, where the vector boson decays leptonically (ATLAS) or hadronically (CMS) and the Higgs boson to $b\bar{b}$ (both experiments), WW or $\tau^+\tau^-$ (CMS). No deviation from the standard model is seen in any of these final states and limits can be placed on the allowed production cross section times branching ratio for resonances between 0.8 and 2.5 TeV, on the parameters of a Minimal Walking Technicolor Model and on a heavy vector triplet model.

Both experiments [99,100] have also searched for resonant production of Higgs boson pairs $X \rightarrow H^0 H^0$ with $H^0 \rightarrow b\bar{b}$. No signal is observed and limits are placed on the possible production cross section for any new resonance.

$Y \rightarrow W/Z + X$ with $X \rightarrow jj$:

ATLAS has searched for a dijet resonance [101] with an invariant mass in the range 130 – 300 GeV, produced in association with a W or a Z boson. The analysis used 20.3 fb^{-1} of data recorded at $\sqrt{s} = 8$ TeV. The W or Z boson is required to decay leptonically ($\ell = e, \mu$). No significant deviation from the standard model prediction is observed and limits are set on the production cross section times branching ratio for a hypothetical technipion produced in association with a W or Z boson from the decay of a technirho particle in the context of Low Scale Technicolor models.

2.3 Vector-like third generation quarks

Vector-like quarks (VLQ) have non-chiral couplings to W bosons, i.e. their left- and right-handed components couple in the same way. They therefore have vectorial couplings to

W bosons. Vector-like quarks arise in Little Higgs theories, top-coloron-models, and theories of a composite Higgs boson with partial compositeness. At the LHC, VLQs can be pair produced, via the dominant gluon-gluon fusion. VLQs can also be produced singly by their electroweak effective couplings to a weak boson and a standard model quark. In the following the notation T quark refers to a vector-like quark with charge $2/3$ and the notation B quark refers to a vector-like quark with charge $-1/3$. T quarks can decay to bW , tZ , or tH^0 . Weak isospin singlets are expected to decay to all three final states with (asymptotic) branching fractions of 50%, 25%, 25%, respectively. Weak isospin doublets are expected to decay exclusively to tZ and to tH^0 [102]. Analogously, B quarks can decay to tW , bZ , or bH^0 .

Searches for T quarks that decay to W , Z and H^0 bosons

$T \rightarrow bW$:

CMS has searched for pair production of heavy T quarks that decay exclusively to bW [103]. The analysis selects events with exactly one charged lepton, assuming that the W boson from the second T quark decays hadronically. Under this hypothesis, a 2-constraint kinematic fit can be performed to reconstruct the mass of the T quark. The two-dimensional distribution of reconstructed mass vs S_T is used to test for the signal. S_T is the scalar sum of the missing p_T and the transverse momenta of the lepton and the leading four jets. At times the hadronically-decaying W boson is produced with a large Lorentz boost, leading to the W decay products merged into a wide single jet also known as a fat jet. Algorithms such as jet pruning [104] are used to resolve the substructure of the fat jets from the decays of the heavy particles. If the mass of the boosted jet is compatible with the W -boson mass, then this W boson candidate jet is used in the kinematic reconstruction of the T quark. No excess over standard model backgrounds is observed. This analysis, when combined with the search in the fully hadronic final state [105] excludes new quarks that decay 100% to bW for masses below 890 GeV [106].

An analogous search has been carried out by ATLAS [109]. It uses the lepton+jets final state with an isolated electron or

muon and at least four jets, at least one of which must be tagged as a b-jet. The selection is optimized for T quark masses above about 400 GeV and requires reconstruction of hadronically decaying W boson, including those with a high boost leading to merged decay products, and large angular separation between the W bosons and the b-jets originating from the decay of the heavy T quark. The analysis focuses on the reconstructed heavy T quark mass from the hadronic W candidate and a b-jet. No significant excess of events above standard model expectation is observed. For $BR(T \rightarrow bW) = 1$, T quark masses lower than 765 GeV are excluded.

$T \rightarrow tH^0$:

ATLAS has performed a search for $T\bar{T}$ production with $T \rightarrow tH^0$ [109]. Given the dominant decay mode $H^0 \rightarrow b\bar{b}$, these events are characterized by a large number of jets, many of which are b-jets. Thus the event selection requires one isolated electron or muon and at least five jets, two of which must be tagged as b-jets. The data are classified according to their jet-multiplicity (five and six-or-more), b-jet multiplicity (2, 3, and ≥ 4) and the invariant mass of the two b-tagged jets with lowest ΔR between the two b-tagged jets (for \geq six jet events). The distribution of H_T , the scalar sum of the lepton and jet p_T s and the missing E_T , for each category is used as the discriminant for the final signal and background separation. No excess of events is found. Weak isospin doublet T quarks are excluded below 855 GeV for $BR(T \rightarrow tH^0) = 1$. The CMS search for $T\bar{T}$ production, with $T \rightarrow tH^0$ decays have been performed in both lepton+jets, multilepton and all hadronic final states. The lepton+jets analysis [110] emphasizes the presence of large number of b-tagged jets, and combines with other kinematic variables in a Boosted Decision Tree (BDT) for enhancing signal to background discrimination. The multilepton analysis [110] optimized for the presence of b-jets and the large hadronic activity. For $BR(T \rightarrow Wb) = 1$, the combined lepton+jets and multilepton analyses lead to a lower limit on T quark masses of 706 GeV. A search for $T \rightarrow tH^0$ in all hadronic decays [111], optimized for a high mass T quark, and based on identifying boosted top quark jets has been carried out

by CMS. This search aims to resolve sub-jets within the fat jet arising from boosted top quark decays, including b-tagging of the sub-jets. A likelihood discriminator is defined based on the distributions of H_T , and the invariant mass of the two b-jets in the events for signal and background. No excess above background expectations is observed. Assuming 100% BR for $T \rightarrow tH^0$, this analysis leads to a lower limit of 745 GeV on the mass of the T quark.

A CMS search for $T \rightarrow tH^0$ with $H^0 \rightarrow \gamma\gamma$ decays has been performed [112]. To identify the Higgs boson produced in the decay of the heavy T quark, and the subsequent $H^0 \rightarrow \gamma\gamma$ decay, the analysis focuses on identification of two photons in events with one or more high p_T lepton+jets or events with no leptons and large hadronic activity. A search for a resonance in the invariant mass distribution of the two photons in events with large hadronic activity defined by the H_T variable shows no excess above the prediction from standard model processes. The analysis results in exclusion of T quark masses below 540 GeV.

$T \rightarrow tZ$:

A targeted search by CMS for T quarks that decay exclusively to tZ based on an integrated luminosity of 1.1 fb^{-1} from pp collisions at $\sqrt{s} = 7 \text{ TeV}$ [107]. Selected events must have three isolated charged leptons, two of which must be consistent with a leptonic Z -boson decay. No significant excess was observed. T quark masses below 485 GeV are excluded. The CMS analysis [110] with combined searches in lepton+jets, dilepton and multilepton final states yields a lower limit on the mass of the T of 782 GeV. A complementary search has been carried out by ATLAS for new heavy quarks decaying into a Z boson and a third generation quark [113], with $T \rightarrow tZ$. Selected events contain a high transverse momentum Z boson that decays leptonically, together with two b-jets, which is modified to require at least one b-tagged jet, for events with additional leptons. No significant excess of events above the standard model expectation is observed. For the weak-isospin singlet scenario, a T quark with mass lower than 655 GeV is

excluded, while for a particular weak-isospin doublet scenario, a T quark with mass lower than 735 GeV is excluded.

The ATLAS experiment has studied the electroweak production of single T quarks, which is accompanied by a b-jet and a light jet [113]. The initial event selection for this search is very similar to that of $T\bar{T}$ production with $T \rightarrow tZ$ decays, and for both the dilepton and trilepton signatures, it requires the presence of an additional energetic jet in the forward region ($2.5 < |\eta| < 4.5$), a characteristic signature of single heavy quark production. An upper limit of 190 fb is obtained for the process $\sigma(pp \rightarrow T\bar{b}q) \times B(T \rightarrow tZ)$ with a heavy T quark mass at 700 GeV. For a specific composite Higgs model [114], the WTb vertex is parameterized by λ_T , which is associated with the Yukawa coupling in the composite sector and the degree of compositeness of the quarks in the 3rd generation. With the current dataset unfortunately the search is not sensitive to $\lambda_T < 1.5$ nor to any values of $V_{Tb} < 1$.

Same-Sign dilepton analyses:

Pair-production of T or B quarks with their antiparticles can result in events with like-sign leptons, for example if the decay $T \rightarrow tH \rightarrow bWW^+W^-$ is present, followed by leptonic decays of two same-sign W bosons. ATLAS and CMS have searched for this final state. The ATLAS search [121] requires two leptons with the same electric charge, at least two jets of which at least one must be tagged as a b-jet, and missing p_T . ATLAS quotes exclusions of some possible branching fraction combinations depending on the mass of the new quarks. T quarks that are electroweak singlets are excluded below 590 GeV (assuming branching fractions to the W , Z , and H^0 decay modes arising from a singlet model). For the same-sign lepton signature, the sensitivity is largest for T quarks that decay exclusively to tH^0 .

Combination $T \rightarrow bW/tZ/tH^0$:

The limits set by ATLAS searches in lepton+jets, dileptons with same-sign charge, and final states with Z boson have been combined and the results obtained for various combinations of branching fractions for T quark decays to bW , tH^0 and tZ are shown in Fig. 1. The combined analysis excludes T

quarks that exclusively decay to bW/tH^0 with masses below 765/950 GeV [109], and sets lower T quark mass limits that range from 715 to 950 GeV for all possible values of the branching fractions to the three decay modes.

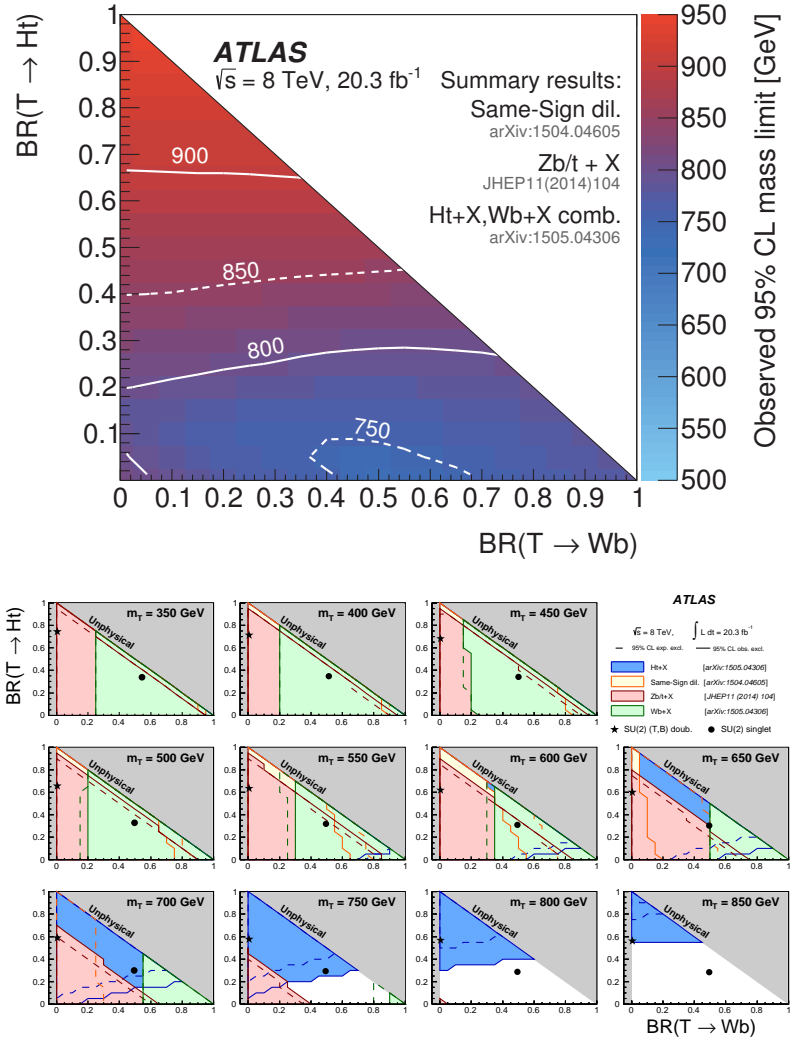


Figure 1: Observed limits on the mass of the T quark in the plane of $BR(T \rightarrow tH^0)$ versus $BR(T \rightarrow bW)$ from all ATLAS searches for TT production [109]. Top panel: summary of the most restrictive observed limit on the mass. Contour lines are provided to guide the eye. Bottom panel: Exclusion limits are drawn sequentially for each of the analyses and overlaid (rather than combined). The circle and star symbols denote the default branching ratios for the weak-isospin singlet and doublet cases.

An inclusive search by CMS targeted at heavy T quarks decaying to any combination of bW , tZ , or tH^0 is described in Ref. [110]. Selected events have at least one isolated charged lepton. Events are categorized according to number and flavour of the leptons, the number of jets, and the presence of hadronic vector boson and top quark decays that are merged into a single jet. The use of jet substructure to identify hadronic decays significantly increases the acceptance for high T quark masses. No excess above standard model backgrounds is observed. Limits on the pair production cross section of the new quarks are set, combining all event categories, for all combinations of branching fractions into the three final states. For T quarks that exclusively decay to $bW/tZ/tH^0$, masses below 700/782/706 GeV are excluded. Electroweak singlet vector-like T quarks which decay 50% to bW , 25% to tZ , and 25% to tH^0 are excluded for masses below 696 GeV (Fig. 2 top panel). This analysis was the first from CMS to obtain limits on the mass of the T quark for all possible values of the branching fractions into the three different final states bW , tZ and tH [110]. A combination [106] of the leptonic inclusive analysis with the targeted $T \rightarrow tH^0$ decays to all-hadronic final state, and $T \rightarrow Wb$ decays with all-hadronic and single-lepton final states with emphasis on bW mass reconstruction, leads to a combined exclusion of T quarks between 790 and 890 GeV and is shown in Fig. 2 (bottom panel). From the combination analyses, any T quark that exclusively decays to $bW/tZ/tH$ is required to have masses above 890/830/840 GeV [106].

Searches B quarks that decay to W , Z and H^0 bosons

ATLAS and CMS have performed searches for pair production of heavy B quarks which subsequently decay to Wt , bZ or bH^0 . The searches have been carried out in final states with single leptons, di-leptons (with same charge or opposite charge), multileptons, as well as in fully hadronic final states.

$B \rightarrow WtX$:

Search for $B \rightarrow tW$ has been performed by the ATLAS experiment [116] using lepton+jets events. This analysis relies on a discriminant obtained via the BDT technique. The BDT uses kinematic and topological variables such as the jet and b -jet

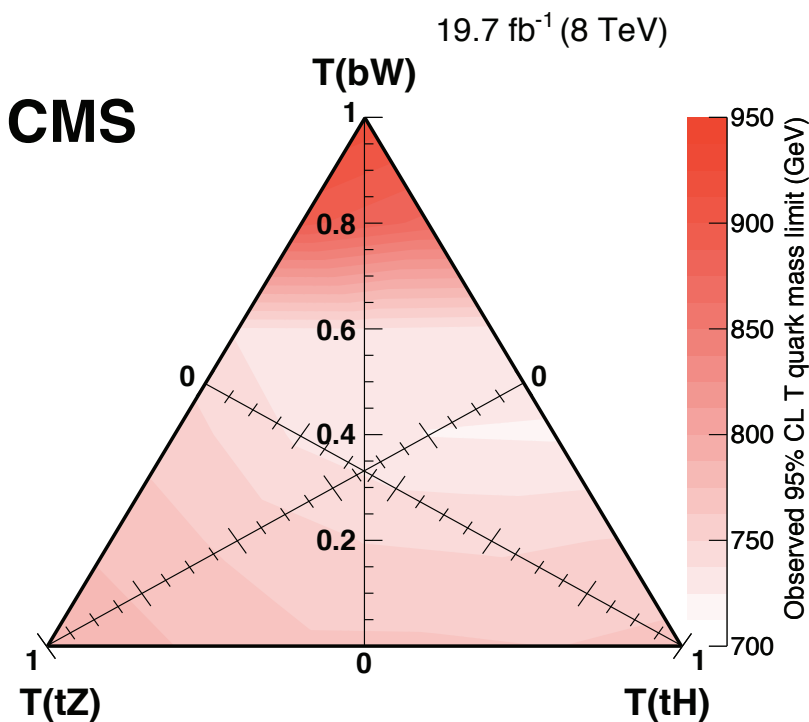
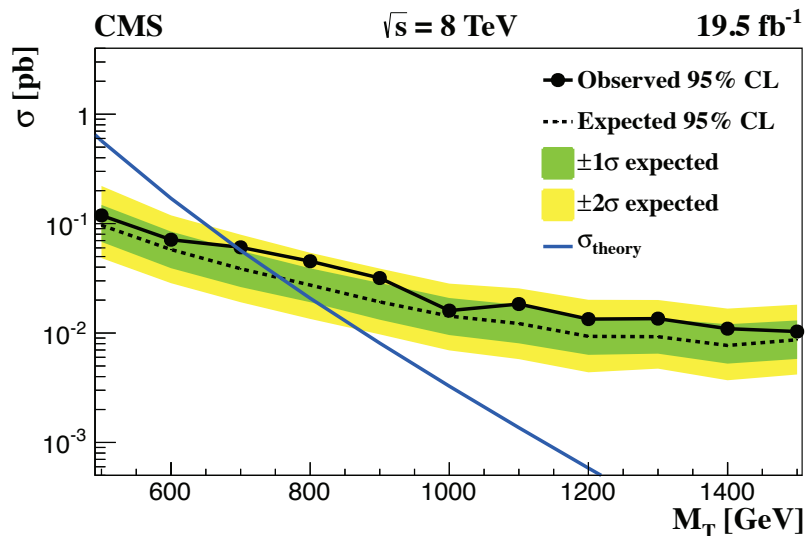


Figure 2: Top panel: upper limit on the T quark production cross section for branching fractions into bW , tH^0 , tZ of 50%, 25%, 25% obtained from the leptonic inclusive analysis [110]. Bottom panel: Branching fraction triangle with observed limits for the T quark mass from the CMS combination analysis [106].

multiplicity, H_T , the angular separation between the lepton and the leading b-tagged jet or between lepton and hadronic W/Z candidates, the transverse mass of the leptonically decaying W boson candidate, p_T of various objects including the leptonically decaying W boson, the number of hadronic W/Z candidates, etc. For $BR(B \rightarrow tW) = 1$, the lower limit on the mass of the B quark is obtained to be 810 GeV. For the weak-isospin singlet scenario, a B quark with mass lower than 640 GeV is excluded. A similar search by CMS [117] selects events with one lepton and four or more jets, with at least one b-tagged jet, significant missing p_T , and further categorizes them based on the number of jets tagged as arising from the decay of boosted W , Z or H^0 bosons. The S_T distributions of the events in different categories show no excess of events above the expected background and yield a lower limit on the B quark mass of 732 GeV for $BR(B \rightarrow Wt) = 1$.

$B \rightarrow bZX$:

A search by CMS [115] for the pair-production of a heavy B quark and its antiparticle, one of which decays to bZ selects events with a Z -boson decay to e^+e^- or $\mu^+\mu^-$ and a jet identified as originating from a b quark. The signal from $B \rightarrow bZ$ decays would appear as a local enhancement in the bZ mass distribution. No such enhancement is found and B quarks that decay 100% into bZ are excluded below 700 GeV. This analysis also sets upper limits on the branching fraction for $B \rightarrow bZ$ decays of 30-100% in the B quark mass range 450-700 GeV. A complementary search has been carried out by ATLAS for new heavy quarks decaying into a Z boson and a b-quark [113]. Selected dilepton events contain a high transverse momentum Z boson that decays leptonically, together with two b-jets. If the dilepton events have an extra lepton in addition to those from the Z boson, then only one b-jet is required. No significant excess of events above the standard model expectation is observed, and mass limits are set depending on the assumed branching ratios, see Fig. 3. In a weak-isospin singlet scenario, a B quark with mass lower than 645 GeV is excluded, while for a particular weak-isospin doublet scenario, a B quark with mass lower than 725 GeV is excluded.

ATLAS has searched for the electroweak production of single B quarks, which is accompanied by a b-jet and a light jet [113]. The dilepton selection for double B production is modified for the single B production study by requesting the presence of an additional energetic jet in the forward region. An upper limit of 200 fb is obtained for the process $\sigma(pp \rightarrow B\bar{b}q) \times B(B \rightarrow Zb)$ with a heavy B quark mass at 700 GeV. This search indicates that the electroweak mixing parameter X_{Bb} below 0.5 is neither expected or observed to be excluded for any values of B quark mass.

Combination $B \rightarrow tW/bZ/bH^0$:

The ATLAS experiment has combined the various analyses targeted for specific decay modes to obtain the most sensitive limits on the pair production of B quarks [109]. The analyses using single lepton events, same sign charge dilepton events, events with opposite sign dilepton events, and multilepton events are combined to obtain lower limits on the mass of the B quark in the plane of $BR(B \rightarrow Wt)$ vs $BR(B \rightarrow bH)$. The searches are optimized for 100% branching fractions and hence are most sensitive at large $BR(B \rightarrow Wt)$, and also at large $BR(B \rightarrow bH^0)$. For all possible values of branching ratios in the three decay modes tW , bZ , or bH^0 , the lower limits on the B quark mass is found to be between 575 GeV and 813 GeV and as shown in Fig. 3.

A similar combination of CMS analyses [115] in the final states with single leptons, di-leptons (with same charge or opposite charge), multileptons, as well as fully hadronic decays lead to results shown in Fig. 4. The discriminating variables used in these analyses are S_T , H_T and the invariant mass of the dileptons and the b-jets. As different topologies target multiple decay modes, with various degree of sensitivity to the B quark mass, the best results for the Wt decays is obtained from the combination of lepton+jets, same-sign dilepton and multilepton events, while for the bZ mode a combination of opposite-sign dilepton and multilepton events leads to the best sensitivity for the mass limits. For the bH^0 decays, the all-hadronic events give the dominant contribution to the mass limit. For B quarks that decay exclusively into tW masses below 880 GeV are

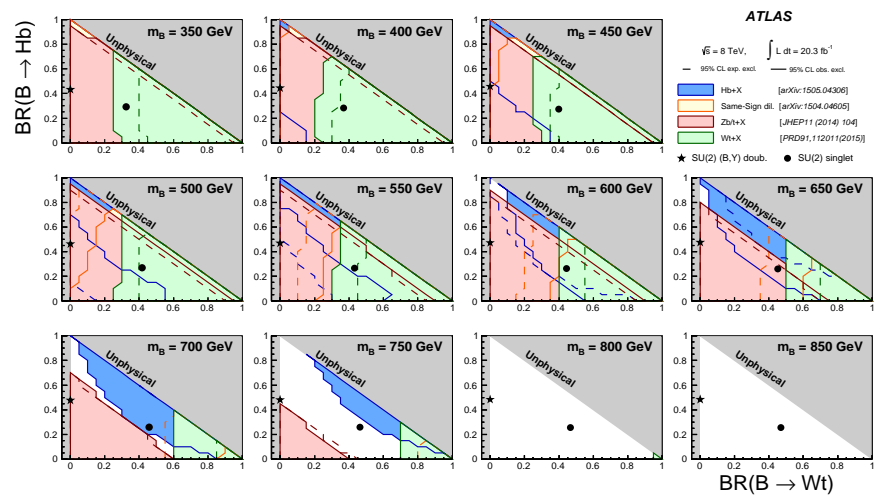
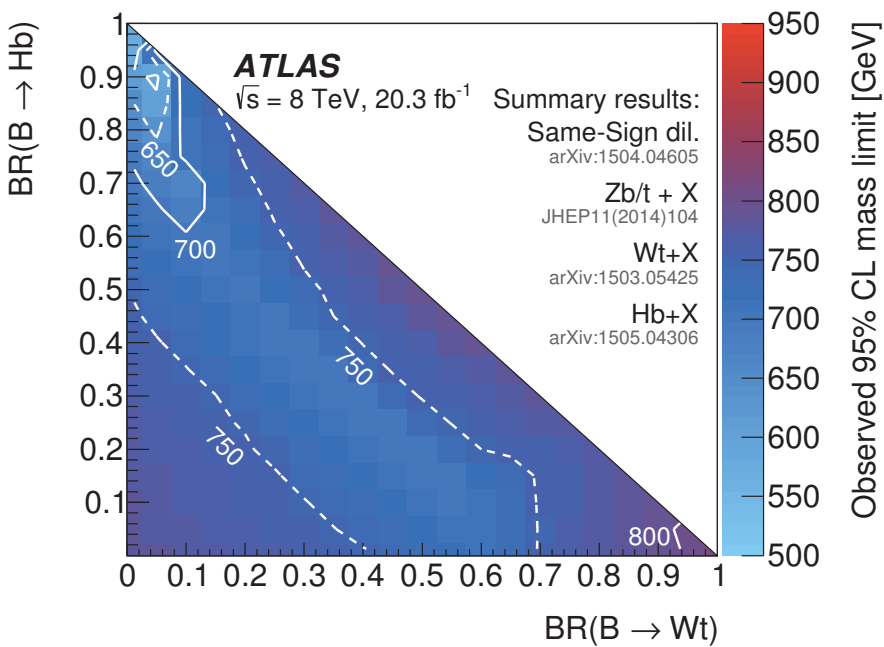


Figure 3: Observed limits on the mass of the T quark in the plane of $BR(B \rightarrow bH^0)$ versus $BR(B \rightarrow tW)$ from all ATLAS searches for BB production [109]. Top panel: summary of the most restrictive observed limit on the mass. Contour lines are provided to guide the eye. Bottom panel: Exclusion limits are drawn sequentially for each of the analyses and overlaid (rather than combined).

excluded, while for 100% decay branching fraction of B to bH^0 , B quarks up to 900 GeV are excluded. The exclusion limits for

all combinations of branching fractions lie between 740 GeV to 900 GeV, and are shown in Fig. 4, together with the cross section limit plotted for B quark decays to the bH^0 mode.

2.4 A charge $+5/3$ top-partner quark

In models of dynamical electroweak symmetry breaking, the same interactions which give rise to the mass of the top-quark can give unacceptably large corrections to the branching ratio of the Z boson to $b\bar{b}$ [75]. These corrections can be substantially reduced, however, in theories with an extended “custodial symmetry” [45]. This symmetry requires the existence of a charge $+5/3$ vector-like partner of the top quark.

Both experiments have performed a search for a heavy top vector-like quark $T_{5/3}$, with exotic charge $5/3$, such as that proposed in Refs. [118,119]. The analyses assume pair-production of $T_{5/3}$ with $T_{5/3}$ decaying with 100% branching fraction to tW . The analysis is based on searching for same-sign leptons, from the two W bosons from one of the $T_{5/3}$. Requiring same-sign leptons eliminates most of the standard model background processes, leaving those with smaller cross sections: $t\bar{t}$, W , $t\bar{t}Z$, WWW , and same-sign WW . In addition backgrounds from instrumental effects due to charge misidentification are considered. The CMS search also utilizes jet substructure techniques to identify boosted $T_{5/3}$ topologies. These searches restrict the $T_{5/3}$ mass to be higher than 800 GeV [120]. The pair-production limits obtained by ATLAS correspond to a lower mass limit on $T_{5/3}$ of 840 GeV [116]

The single $T_{5/3}$ production cross section depends on the coupling constant λ of the $tWT_{5/3}$ vertex. ATLAS has performed an analysis of same-sign dileptons which includes both the single and pair production. This analysis leads to a lower limit on the mass of the $T_{5/3}$ of 750 GeV for both values of $\lambda = 0.5$ and 1.0 [121].

2.5 Colorons and Colored Scalars

These particles are associated with top-condensate and top-seesaw models, which involve an enlarged color gauge group. The new particles decay to dijets, $t\bar{t}$, and $b\bar{b}$.

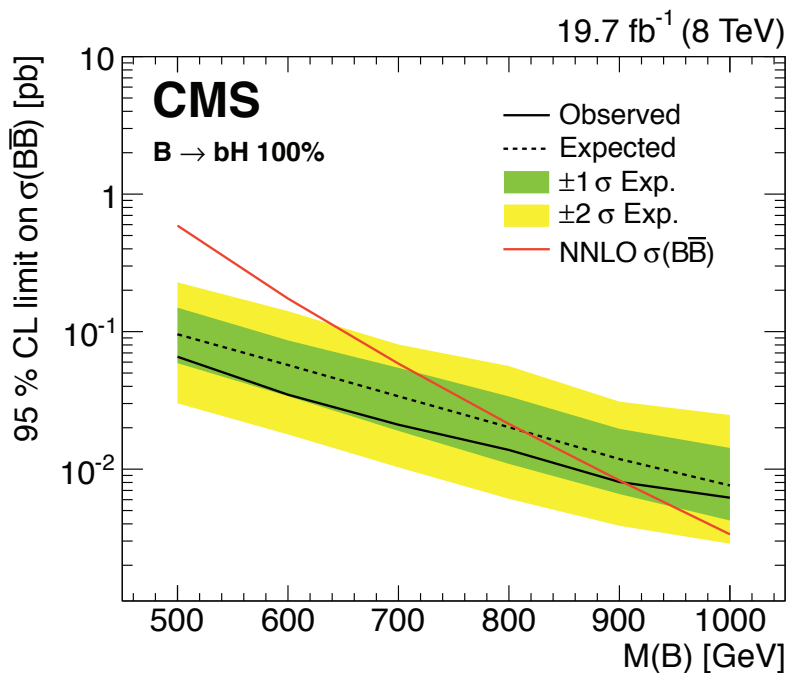
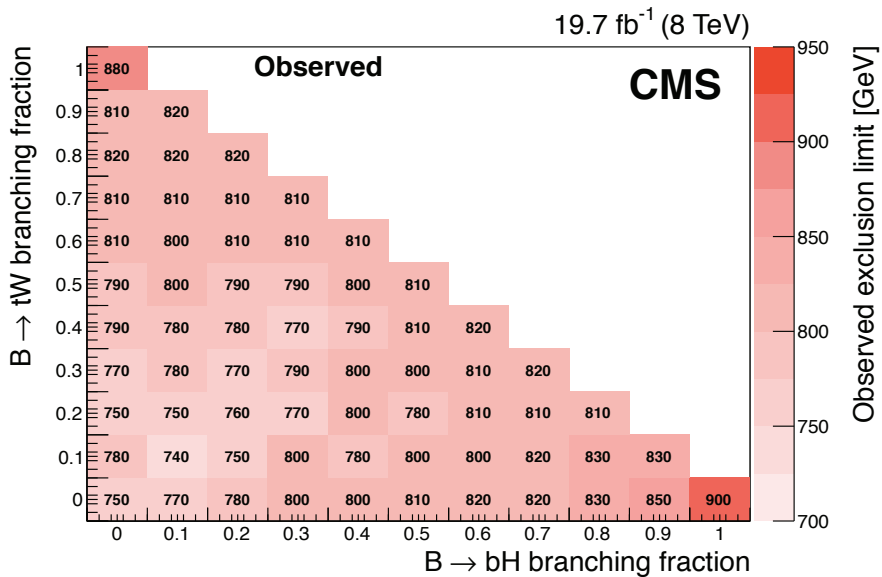


Figure 4: Top panel: observed limits on the B quark mass for each combination of branching fractions to tW , bZ , and bH^0 obtained by the combination of channels. The color scale represents the mass exclusion limit obtained at each point [115]. Bottom panel: Observed and expected cross section limit results as a function of B mass, for the combination of all channels and for exclusive branching fraction of B to bH [115].

Direct searches for colorons, color-octet scalars and other heavy objects decaying to $q\bar{q}$, qg , qq , or gg has been performed using LHC data from pp collisions at $\sqrt{s}=7$ and 8 TeV. Based on the analysis of dijet events from a data sample corresponding to a luminosity of 19.6 fb^{-1} , the CMS experiment excludes pair production of colorons with mass between $1.20 - 3.60$ and $3.90 - 4.08$ TeV at 95% C.L. as shown in Fig. 5 [83]. A search for pair-produced colorons based on an integrated luminosity of 5.0 fb^{-1} at $\sqrt{s} = 7$ TeV by CMS excludes colorons with masses between 250 GeV and 740 GeV, assuming colorons decay 100% into $q\bar{q}$ [122]. This analysis is based on events with at least four jets and two dijet combinations with similar dijet mass. Color-octet scalars (s8) with masses between $1.20 - 2.79$ TeV are excluded by CMS (Fig. 5 [83]), and below 2.7 TeV by ATLAS [82].

These studies have now been extended to take advantage of the increased center-of-mass energy during Run 2 of the LHC. Using the 40pb^{-1} of data collected at $\sqrt{s} = 13$ TeV, searches for narrow resonances have been performed by CMS. An analysis of the dijet invariant mass spectrum formed using wide jets [123], separated by $\Delta\eta_{jj} \leq 1.3$, leads to limits on new particles decaying to parton pairs (qq , qg , gg). Specific exclusions on the masses of colorons and color-octet scalars are obtained and shown in Fig. 5.

3. Conclusions

As the above analyses have demonstrated, there is already substantial sensitivity to possible new particles predicted to accompany the H^0 in dynamical frameworks of electroweak symmetry breaking. No hints of any deviations from the standard model have been observed, and limits typically at the scale of a few hundred GeV to 1 TeV are set.

Given the need to better understand the H^0 and to determine in detail how it behaves, we expect that such analyses will be a major theme of Run 2 the LHC, and we look forward to increased sensitivity as a result of the higher luminosity at the increased centre of mass energy of collisions.

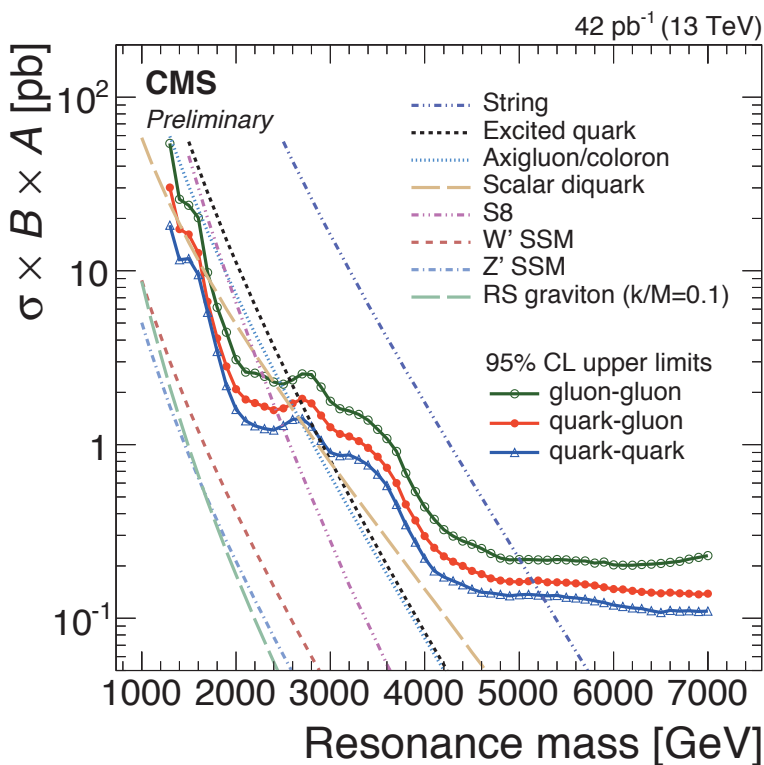
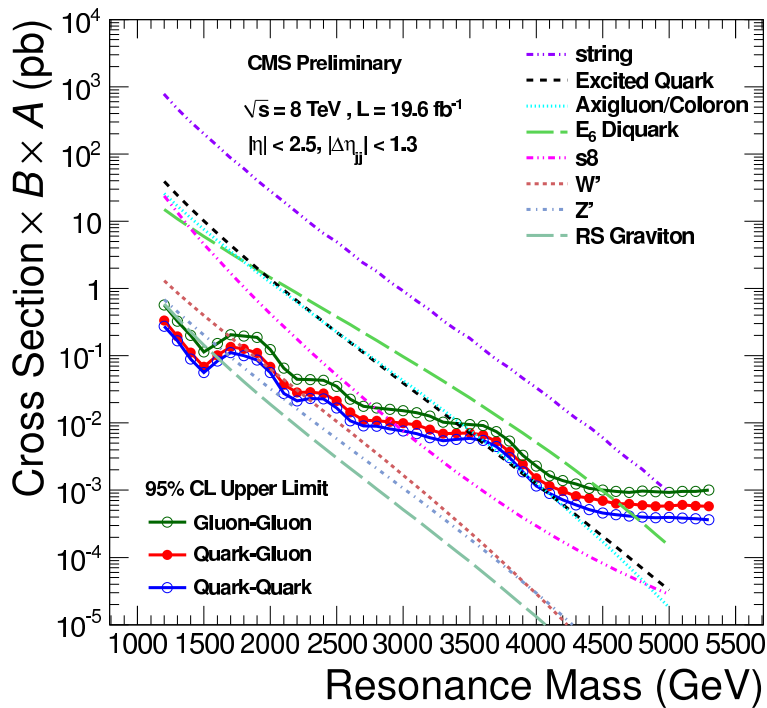


Figure 5: Observed 95% C.L. limits on $\sigma \times B \times A$ for string resonances, excited quarks, axigluons, colorons, E_6 diquarks, s8 resonances, W' and Z' bosons, and Randall-Sundrum gravitons g_{KK} . Top panel: results from Ref. [83] from Run 1. Bottom panel: results from Ref. [123] from Run 2.

References

1. ATLAS Collab., Phys. Lett. **B716**, 1 (2012).
2. CMS Collab., Phys. Lett. **B716**, 30 (2012).
3. S. Weinberg, Physica A **96**, 327 (1979).
4. A. Manohar and H. Georgi, Nucl. Phys. **B234**, 189 (1984).
5. H. Georgi, Nucl. Phys. **B266**, 274 (1986).
6. R.S. Chivukula, hep-ph/0011264 (2000).
7. R.S. Chivukula, M.J. Dugan, and M. Golden, Phys. Rev. **D47**, 2930 (1993).
8. S. Weinberg, Phys. Rev. **D13**, 974 (1976).
9. S. Weinberg, Phys. Rev. **D19**, 1277 (1979).
10. L. Susskind, Phys. Rev. **D20**, 2619 (1979).
11. K. Lane, hep-ph/0202255 (2002).
12. C.T. Hill and E.H. Simmons, Phys. Reports **381**, 235 (2003), [Erratum-ibid. **390**, 553 (2004)].
13. R. Shrock, hep-ph/0703050 (2007).
14. E. Eichten *et al.*, Rev. Mod. Phys. **56**, 579 (1984) [Addendum-ibid. **58**, 1065 (1986)].
15. E. Eichten *et al.*, Phys. Rev. **D34**, 1547 (1986).
16. R.S. Chivukula and V. Koulovassilopoulos, Phys. Lett. **B309**, 371 (1993).
17. R. Foadi, M.T. Frandsen, and F. Sannino, Phys. Rev. **D87**, 095001 (2013).
18. B. Holdom, Phys. Lett. **B150**, 301 (1985).
19. K. Yamawaki, M. Bando, and K.-i. Matumoto, Phys. Rev. Lett. **56**, 1335 (1986).
20. T.W. Appelquist, D. Karabali, and L.C.R. Wijewardhana, Phys. Rev. Lett. **57**, 957 (1986).
21. T. Appelquist and L.C.R. Wijewardhana, Phys. Rev. **D35**, 774 (1987).
22. T. Appelquist and L.C.R. Wijewardhana, Phys. Rev. **D36**, 568 (1987).
23. E. Gildener and S. Weinberg, Phys. Rev. **D13**, 3333 (1976).
24. Z. Chacko, R. Franceschini and R. K. Mishra, JHEP **1304**, 015 (2013).
25. B. Bellazzini *et al.*, Eur. Phys. J. **C73**, 2333 (2013).
26. B. Bellazzini *et al.*, Eur. Phys. J. **C74**, 2790 (2014).
27. Z. Chacko, R.K. Mishra, and D. Stolarski, JHEP **1309**, 121 (2013).

28. J.R. Ellis, M.K. Gaillard, and D.V. Nanopoulos, Nucl. Phys. **B106**, 292 (1976).
29. M.A. Shifman *et al.*, Sov. J. Nucl. Phys. **30**, 711 (1979) [Yad. Fiz. **30**, 1368 (1979)].
30. A.I. Vainshtein, V.I. Zakharov, and M.A. Shifman, Sov. Phys. Usp. **23**, 429 (1980) [Usp. Fiz. Nauk **131**, 537 (1980)].
31. M. Bando, K.-i. Matumoto, and K. Yamawaki, Phys. Lett. **B178**, 308 (1986).
32. W.D. Goldberger, B. Grinstein, and W. Skiba, Phys. Rev. Lett. **100**, 111802 (2008).
33. S. Matsuzaki and K. Yamawaki, Phys. Rev. **D85**, 095020 (2012).
34. S. Matsuzaki and K. Yamawaki, Phys. Rev. **D86**, 035025 (2012).
35. E. Eichten, K. Lane, and A. Martin, arXiv:1210.5462 (2012).
36. D.B. Kaplan and H. Georgi, Phys. Lett. **B136**, 183 (1984).
37. D.B. Kaplan, H. Georgi, and S. Dimopoulos, Phys. Lett. **B136**, 187 (1984).
38. M.E. Peskin, Nucl. Phys. **B175**, 197 (1980).
39. J. Preskill, Nucl. Phys. **B177**, 21 (1981).
40. R. Barbieri and A. Strumia, hep-ph/0007265 (2000).
41. N. Arkani-Hamed, A.G. Cohen, and H. Georgi, Phys. Lett. **B513**, 232 (2001).
42. N. Arkani-Hamed *et al.*, JHEP **0208**, 020 (2002).
43. N. Arkani-Hamed *et al.*, JHEP **0207**, 034 (2002).
44. M. Schmaltz and D. Tucker-Smith, Ann. Rev. Nucl. and Part. Sci. **55**, 229 (2005).
45. K. Agashe *et al.*, Phys. Lett. **B641**, 62 (2006).
46. P. Sikivie *et al.*, Nucl. Phys. **B173**, 189 (1980).
47. R.S. Chivukula, A.G. Cohen, and K.D. Lane, Nucl. Phys. **B343**, 554 (1990).
48. B. Bellazzini, C. Csaki, and J. Serra, Eur. Phys. J. **C74**, 2766 (2014).
49. V.A. Miransky, M. Tanabashi, and K. Yamawaki, Phys. Lett. **B221**, 177 (1989) and Mod. Phys. Lett. **A4**, 1043 (1989).
50. W.A. Bardeen, C.T. Hill, and M. Lindner, Phys. Rev. **D41**, 1647 (1990).
51. C.T. Hill, Phys. Lett. **B266**, 419 (1991).

52. B.A. Dobrescu and C.T. Hill, Phys. Rev. Lett. **81**, 2634 (1998).
53. R.S. Chivukula *et al.*, Phys. Rev. **D59**, 075003 (1999).
54. S. Dimopoulos and L. Susskind, Nucl. Phys. **B155**, 237 (1979).
55. E. Eichten and K.D. Lane, Phys. Lett. **B90**, 125 (1980).
56. D.B. Kaplan, Nucl. Phys. **B365**, 259 (1991).
57. T. Appelquist, M. Piai, and R. Shrock, Phys. Rev. **D69**, 015002 (2004).
58. R.S. Chivukula, B.A. Dobrescu, and E.H. Simmons, Phys. Lett. **B401**, 74 (1997).
59. Y. Grossman and M. Neubert, Phys. Lett. **B474**, 361 (2000).
60. S.J. Huber and Q. Shafi, Phys. Lett. **B498**, 256 (2001).
61. T. Gherghetta and A. Pomarol, Nucl. Phys. **B586**, 141 (2000).
62. K. Agashe, R. Contino, and A. Pomarol, Nucl. Phys. **B719**, 165 (2005).
63. G.F. Giudice *et al.*, JHEP **0706**, 045 (2007).
64. R.S. Chivukula and H. Georgi, Phys. Lett. **B188**, 99 (1987).
65. G. D'Ambrosio *et al.*, Nucl. Phys. **B645**, 155 (2002).
66. K. Agashe *et al.*, hep-ph/0509117 (2005).
67. T. Appelquist and R. Shrock, Phys. Lett. **B548**, 204 (2002).
68. B. Keren-Zur *et al.*, Nucl. Phys. **B867**, 429 (2013).
69. J.M. Maldacena, Adv. Theor. Math. Phys. **2**, 231 (1998).
70. For a review, see C. Csaki, J. Hubisz, and P. Meade, hep-ph/0510275 (2005), and “Extra Dimensions” review in this volume.
71. E.T. Neil, PoS LATTICE **2011**, 009 (2011).
72. J. Giedt, PoS LATTICE **2012**, 006 (2012).
73. J. Kuti, PoS LATTICE **2013**, 004 (2014).
74. T. Appelquist *et al.*, arXiv:1309.1206 [hep-lat].
75. R.S. Chivukula, S.B. Selipsky, and E.H. Simmons, Phys. Rev. Lett. **69**, 575 (1992).
76. ATLAS Collab., Phys. Rev. **D90**, 052005 (2014).
77. CMS Collab., JHEP **1504**, 025 (2015).
78. ATLAS Collab., JHEP **1507**, 157 (2015).
79. CMS Collab., CMS-PAS-EXO-12-046 (2015).

80. ATLAS Collab., CERN-PH-EP-2015-090 (2015), to be published in JHEP.
81. CMS Collab., CMS-B2G-13-008 (2015), submitted to PRD.
82. ATLAS Collab., Phys. Rev. **D91**, 052007 (2015).
83. V. Khachatryan *et al.* [CMS Collab.], Phys. Rev. **D91**, 052009 (2015).
84. ATLAS Collab., ATLAS-CONF-2013-060 (2013).
85. ATLAS Collab., JHEP **1409**, 037 (2014).
86. CMS Collab., CERN-PH-EP-2015-190 (2015).
87. ATLAS Collab., Phys. Lett. **B743**, 235 (2015).
88. ATLAS Collab., Eur. Phys. J. **C75**, 165 (2015).
89. ATLAS Collab., Phys. Lett. **B737**, 223 (2014).
90. CMS Collab., Phys. Lett. **B740**, 83 (2015).
91. ATLAS Collab., Eur. Phys. J. **C75**, 209 (2015).
92. ATLAS Collab., Eur. Phys. J. **C75**, 69 (2015).
93. CMS Collab., JHEP **1408**, 174 (2014).
94. ATLAS Collab., CERN-PH-EP-2015-115 (2015).
95. CMS Collab., JHEP **1408**, 173 (2014).
96. ATLAS Collab., Eur. Phys. J. **C75**, 263 (2015).
97. CMS Collab., CERN-PH-EP-2015-096 (2015), submitted to JHEP.
98. CMS Collab., Phys. Lett. **B748**, 255 (2015).
99. ATLAS Collab., Eur. Phys. J. **C75**, 412 (2015).
100. CMS Collab., CMS-EXO-12-053 (2015).
101. ATLAS Collab., ATLAS-CONF-2013-074 (2013).
102. F. del Aguila *et al.*, Nucl. Phys. **B334**, 1 (1990).
103. CMS Collab., CMS-PAS-B2G-12-017 (2014).
104. S.D. Ellis, C.K. Vermilion, and J.R. Walsh, Phys. Rev. **D80**, 051501 (2009).
105. CMS Collab., CMS-PAS-B2G-12-013 (2015).
106. CMS Collab., submitted to PRD, arXiv:1509.04177.
107. CMS Collab., Phys. Rev. Lett. **107**, 271802 (2011).
108. CMS Collab., Phys. Lett. **B718**, 307 (2012).
109. ATLAS Collab., JHEP **1508**, 105 (2015).
110. CMS Collab., Phys. Lett. **B729**, 149 (2014).
111. CMS Collab., JHEP **1506**, 080 (2015).
112. CMS Collab., cds.cern.ch/record/1709129 (2014).
113. ATLAS Collab., JHEP **1411**, 104 (2014).

114. N. Vignaroli, Phys. Rev. **D86**, 075017 (2012).
115. CMS Collab., submitted to PRD, arXiv:1507.07129.
116. ATLAS Collab., Phys. Rev. **D91**, 112011 (2015).
117. CMS Collab., CMS-PAS-B2G-12-019 (2012),
<http://cds.cern.ch/record/1599436>.
118. R. Contino and G. Servant, JHEP **0806**, 026 (2008).
119. J. Mrazek, A. Wulzer, Phys. Rev. **D81**, 075006 (2010).
120. CMS Collab., Phys. Rev. Lett. **112**, 171801 (2014).
121. ATLAS Collab., JHEP **1510**, 150 (2015).
122. CMS Collab., Phys. Rev. Lett. **110**, 141802 (2013).
123. CMS Collab., CMS-PAS-EXO-15-001 (2015),
<https://cds.cern.ch/record/2048099>.